Macromolecules

pubs.acs.org/Macromolecules Article

Miniemulsion SI-ATRP by Interfacial and Ion-Pair Catalysis for the Synthesis of Nanoparticle Brushes

Rongguan Yin,[‖] Paweł Chmielarz,*[,‖] Izabela Zaborniak, Yuqi Zhao, Grzegorz Szczepaniak, Zongyu Wang, Tong Liu, Yi Wang, Mingkang Sun, Hanshu Wu, Jirameth Tarnsangpradit, Michael R. Bockstaller, and Krzysztof Matyjaszewski*

Cite This: *Macromolecules* 2022, 55, 6332–6340 Read Online

ACCESS | Metrics & More | Article Recommendations | Supporting Information

ABSTRACT: Densely grafted polymer/inorganic nanoparticle hybrids were synthesized *via* a surface-initiated activator regenerated by electron transfer (SI-ARGET) atom transfer radical polymerization (ATRP) of *n*-butyl acrylate (BA) under ion-pair and interfacial catalysis in miniemulsion (hydrodynamic diameters from 105 to 128 nm) with ascorbic acid (AsAc) as the reducing agent. The use of a single-catalyst system in dispersed media allowed the preparation of hybrid materials using a very low catalyst loading (as low as 100 ppm of $[Br\text{-}Cu^{II}(L)]^+$ relative to monomer) and obtaining high monomer conversion (up to 70%) without macroscopic gelation. The resulting polymers exhibited narrow molecular weight distributions ($Đ \leq 1.31$), and the polymer-grafted nanoparticles showed excellent size uniformity. Dispersions in organic solvents (*e.g.*, tetrahydrofuran) were stable without any particle aggregations. Subsequent chain extension of the particle brushes with *tert*-butyl acrylate (*t*BA) proved the livingness of the polymerization and high retention of chain-end fidelity. The developed miniemulsion SI-ARGET ATRP technique with interfacial and ion-pair catalysis offers numerous advantages for the preparation of nanoparticle brushes over the traditional hydrophobic ATRP process. These include a high monomer conversion, high grafting density, better control over polymerization rate, high chain-end livingness, and the use of a very low amount of copper catalyst.

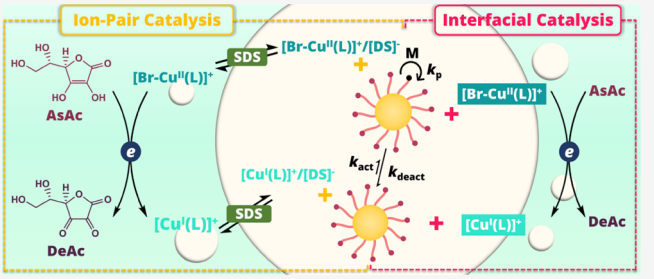

INTRODUCTION

Recent advances in macromolecular chemistry enable the preparation of well-defined organic–inorganic hybrid materials.[1−5] These materials are mostly surface-modified silica nanoparticles (NPs) with tethered organic polymers, forming silica–polymer core/shell nanohybrids.[6−10] Control over the (co)polymer brushes (monomer types,[11,12] brush length,[13] dispersity,[14−16] compositions,[17] *etc.*) attached to the inorganic particle surface results in precisely controlled nanocomposite materials. They display self-organized,[18,19] nanostructured morphologies[20−22] with properties suitable for use in a variety of electrical,[23,24] biomedical,[25,26] optical,[27,28] or mechanical applications.[29,30] With the elaborate design, particle brushes can have excellent thermal stability, rigidity, physical, and chemical resistance.[3,7]

The preparation of dense layers of "monodisperse" polymer chains attached to an inorganic surface requires well-controlled synthetic "grafting from" methods.[3,31] In particular, surface-initiated atom transfer radical polymerization (SI-ATRP),[32−34] one of the most versatile reversible-deactivation radical polymerization (RDRP) processes,[35−37] has been extensively applied to "grafting from" procedures. SI-ATRP enables the preparation of nano-sized core–shell hybrid silica NPs with a controlled thickness of the tethered polymeric shell, predetermined molecular weight (MW), and degree of polymerization (DP) of the tethered chains, low dispersity ($Đ = M_w/M_n$), and high grafting density (σ, chains nm^{-2}).[6,38]

The development of the activator regeneration by electron transfer (ARGET) ATRP technique has enabled the reduction of the copper concentration to ppm levels.[39,40] This method is based on the regeneration of an activator with a reducing agent such as ascorbic acid (AsAc),[41] hydrazine,[42,43] glucose,[39] amines,[44,45] phenols,[46] tin(II) 2-ethylhexanoate,[39] or metal (alloys) such as Ag[47,48] and eutectic gallium indium (EGaIn).[49] The diminishing of the Cu catalyst loading in the polymerization process[50,51] is crucial since even low metal contamination can have a negative impact on the optical, photothermal, or dielectric properties of hybrid materials.[32,38]

One of the biggest challenges in the synthesis of densely grafted polymer brushes from NPs is to avoid macroscopic gelation caused by intermolecular brush coupling. Therefore,

Received: May 29, 2022
Revised: July 13, 2022
Published: July 22, 2022

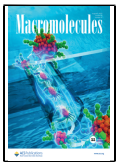

https://doi.org/10.1021/acs.macromol.2c01114
Macromolecules 2022, 55, 6332–6340

Scheme 1. Proposed Mechanism of Miniemulsion SI-ARGET ATRP Triggered by Ascorbic Acid under Ion-Pair and Interfacial Catalysis Conditions

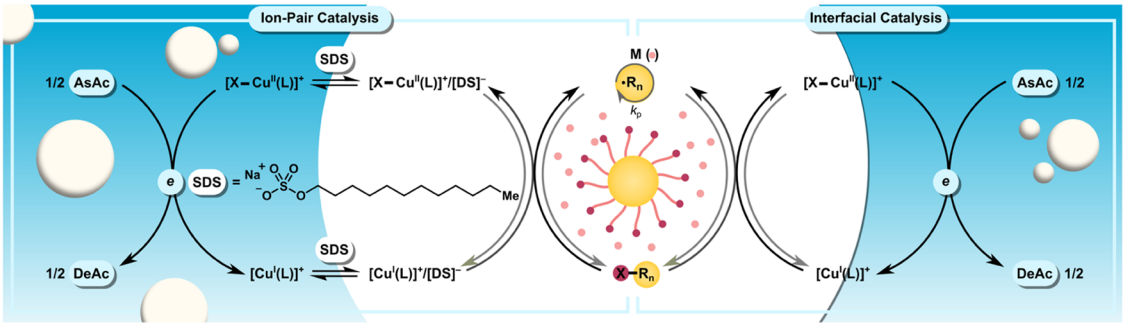

such reactions are typically conducted in the presence of an unbound "sacrificial" initiator,[52] over long polymerization time,[34] at high dilution,[53] and under high pressure[54] or stopped at low monomer conversions.[16,38] Moreover, these procedures may require an additional purification process to remove linear polymer, unreacted monomer, solvent, and significant amounts of the metal catalyst. An alternative approach to suppress cross-coupling, and thus macroscopic gelation, is to create physical boundaries and force polymerization inside a miniemulsion with very small compartments where polymerization occurs directly in separate droplets.[55,56] This approach was adopted for the synthesis of hybrid materials *via* activators generated by electron transfer (AGET) ATRP of *n*-butyl acrylate (BA) from surface-modified silica NPs in a heterogeneous miniemulsion system.[57] However, the need for large amounts of Cu catalyst, typically in the range of thousands of ppm, hinders the practical use of AGET ATRP since it might require tedious and expensive purification.[58,59] Therefore, we developed a unique single-catalyst system for low-ppm ATRP based on a hydrophilic complex, $[Br-Cu^{II}(TPMA)]^+$ (TPMA = tris(2-pyridylmethyl)amine).[60,61] The cationic copper catalyst complex $[Br-Cu^{II}(TPMA)]^+$/anionic surfactant (sodium dodecyl sulfate, SDS) system generated neutral ion pair, $[Br-Cu^{II}(TPMA)]^+/[DS]^-$ (DS = dodecyl sulfate), which predominantly placed the catalyst not only at the interfaces but also inside the hydrophobic monomer droplets, thus allowing a well-controlled polymerization. This method could be relevant for industrial applications since 95% of the catalyst was bound at the water/oil interface, whereas only ∼1% was inside droplets as ion pairs and ∼4% was in the aqueous phase.[61]

The potential advantage of applying a single-catalyst miniemulsion SI-ARGET ATRP to a particle brush system is the possibility to prepare hybrid materials for specialized applications such as optical devices with minimal catalyst contamination. Moreover, the reduced reaction temperature and high monomer conversion make particle brush synthesis more practical. Herein, we present a highly efficient miniemulsion SI-ARGET ATRP technique. The well-defined poly(*n*-butyl acrylate) (PBA) and poly(*n*-butyl acrylate)-*block*-poly(*tert*-butyl acrylate) (PBA-*b*-P*t*BA) brushes were grafted from the surface of silica NPs *via* ion pair and interfacial catalysis at low catalyst concentration using AsAc as the reducing agent (Scheme 1). The effect of AsAc and Cu concentration on the polymerization process was investigated. Ultrasonication used to form a miniemulsion led to the formation of hydroxyl radicals initiating new polymer chains. The use of methyl benzoylformate (MBF) as a hydroxyl radical scavenger suppressed the formation of the linear polymers, provided particle brushes with high monomer conversion, enhanced control over polymerization rate, and high chain-end fidelity.

RESULTS AND DISCUSSION

The hydrophilic copper catalyst was tested at varying concentrations in SI-ARGET ATRP with 22 vol % BA, hexadecane, surface-modified silica NPs (SiO_2−Br) in the organic phase, and the anionic surfactant SDS in aqueous media. Ultrasonication was used to form a miniemulsion with the typical composition reported in Table 1 and additional experimental data in Table 2. Bare silica NPs with an average diameter D_{core} ∼ 15.8 nm were modified by tethering 3-(chlorodimethylsilyl)propyl α-bromoisobutyrate initiators to their surface.[38] The accessible initiator densities of the functionalized nanoparticles in this work were around 0.75 nm^{-2}.[18] Since $[Br-Cu^{II}(TPMA)]^+$ could easily dissociate to $[Cu^{II}(TPMA)]^{2+}$ and Br^- in the aqueous phase, NaBr (0.1 M) was added to the reaction medium to suppress this process.[62,63] The appropriate amount of AsAc was injected dropwise during the polymerization, considering that efficient reduction of Cu^{II} required a ratio of $[AsAc]/[Cu^{II}Br_2]$ = 1.5 (Table S1; additional experimental data in the Supporting Information). After the polymerizations were completed, the silica cores were etched with hydrofluoric acid to prepare untethered polymer chains for size-exclusion chromatography

Table 1. Compositions of Organic and Aqueous Phases in a Typical Miniemulsion SI-ARGET ATRP[a]

component	weight (g)	comments
	Organic Phase	
monomer (BA)	3.13	22 vol %
SiO_2−Br	0.105	$[BA]_0/[SiO_2-Br]_0$ = 1100:1
hexadecane (HD)	0.338	10.8 wt % to monomer
	Aqueous Phase	
water	11.9	18.2 MΩ·cm ultrapure water
SDS	0.194	6.2 wt % to monomer
NaBr	0.164	$[NaBr]_0$ = 0.1 M
$Cu^{II}Br_2$[b]	4.1×10^{-3}	750 ppm compared to monomer
TPMA[b]	0.0106	$[Cu^{II}Br_2]_0/[TPMA]_0$ = 1:2
AsAc[b]	1.6×10^{-3}	slow feeding at 0.5 equiv (to $Cu^{II}Br_2$) per hour

[a]Polymerization conditions: T = 65 °C, t = 3 h. The miniemulsion was prepared by probe ultrasonication as described in the Supporting Information. [b]Values vary according to different reaction entries.

https://doi.org/10.1021/acs.macromol.2c01114
Macromolecules 2022, 55, 6332−6340

Table 2. Miniemulsion ARGET ATRP of BA Grafting from Silica NPs with Different Copper Loadings[a]

entry	$[Cu^{II}Br_2]_0$ (ppm)	k_p^{app} (h^{-1})[b]	conv. (%)[b]	$M_{n,th}$ ($\times10^3$)[c]	$M_{n,app}$ ($\times10^3$)[d]	$Đ$[d]	$d_{Z\text{-ave}}$ (nm)[e]	f_{ino} (%)[f]	σ (nm^{-2})[g]
1	1100	0.221	48	68.5	51.6	1.17	105 ± 1	6.5	0.97
2	750	0.228	50	70.1	48.0	1.29	128 ± 1	6.3	1.07
3	400	0.213	47	66.8	53.5	1.31	117 ± 1	7.6	0.79
4	100	0.205	46	65.0	50.3	1.26	113 ± 1	8.2	0.78
5	75	0.079	21	30.0	23.8	1.58	112 ± 1	21.9	0.52
6	50	0.072	19	27.5	25.6	1.90	121 ± 1	22.0	0.48
7	10	0.066	18	25.6	71.1	2.07	124 ± 1	15.1	0.28
8	1	0.065	18	25.3	204.0	2.30	124 ± 1	8.7	0.18
9	0.01	0.052	14	20.7	705.6	1.86	118 ± 1	6.2	0.07

[a]General reaction conditions: SI-ARGET ATRP of BA 3.5 mL (22% vol) in H_2O, $[BA]_0/[SiO_2{-}Br$, ≈0.75 $Br/nm^2]_0/[Cu^{II}Br_2]_0/[TPMA]_0$ = 1100:1:*x*:2*x*, $[HD]_0$ = 10.8 wt % relative to BA, $[NaBr]_0$ = 0.1 M, $[SDS]_0$ = 6.2 wt % relative to BA, $[AsAc]/[Cu^{II}Br_2]_0$ = 1.5 (AsAc injected using syringe pump, rate = 0.5 equiv h^{-1}), the miniemulsion was prepared by ultrasonication; T = 65 °C, t = 3 h. [b]The slope of the $\ln([M]_0/[M])$ *vs* time plot, calculated from monomer conversion, which was measured by ^1H NMR. [c]$M_{n,th} = ([M]_0/[I]_0) \times \text{conversion} \times M_{monomer} + M_{initiator}$. [d]Apparent M_n and $Đ$ were determined from polymer chains cleaved from silica NPs by hydrofluoric acid (HF) etching using tetrahydrofuran (THF) gel permeation chromatography (GPC) with polystyrene standards. [e]*Z*-average miniemulsion droplet diameter ($d_{Z\text{-ave}}$) measured by DLS during polymerization. [f]Inorganic fraction was determined by TGA. [g]Grafting density (σ) was calculated from eq S1.

(SEC) measurements. Additionally, purified particle brush products were characterized by thermogravimetric analysis (TGA), dynamic light scattering (DLS), and transmission electron microscopy (TEM).

Characterization of Miniemulsion Droplets. In a model heterogeneous miniemulsion system composed of monomer, water, catalyst, and surfactant, emulsion droplets with a hydrodynamic diameter of *ca.* 118 nm (measured by DLS; Figure S1a) were formed, comparable to typical miniemulsion droplets with a diameter of *ca.* 100 nm.[60,61] The fraction of silica NPs inside each droplet ($N_{SiO_2/MD}$) was determined by comparing the total number of silica NPs (N_{SiO_2}) in the oil phase to the total number of miniemulsion droplets in dispersed media (N_{MD}), according to the detailed procedure described (Supporting Information, eq S2). The average number of silica NPs inside each miniemulsion droplet ($N_{SiO_2/MD}$) was estimated to be around 5, which could be observed as 6−7 in typical droplets by TEM analysis (Figure S1b).

Effect of the AsAc Amount and Its Feeding Procedure on Miniemulsion SI-ARGET ATRP of BA Grafting from Silica NPs. Ascorbic acid is a strong reducing agent that rapidly converts Cu^{II} to Cu^{I} species.[64] The fast reduction process diminishes the deactivator $[Br{-}Cu^{II}(TPMA)]^+$ concentration, decreasing control over polymerization. Therefore, an appropriate selection of the AsAc concentration and feeding rate is crucial for ARGET ATRP. The effect of the AsAc concentration and feeding on the polymerization of BA was investigated (Table S1). The ratio of $[AsAc]/[Cu^{II}Br_2(TPMA)]$ was varied from 0.5, 1.0, to 1.5 in total by slow feeding *via* a syringe pump. In addition, an alternative feeding procedure was also investigated by injecting 0.5 equiv AsAc every hour. No measurable effect of the AsAc addition on the micellization of SDS was observed across the tested concentration range. Similar to our previous studies,[61] the faster reduction rate provided faster polymerization (Table S1, entries 1−3). This is attributed to the faster regeneration of the activators and higher concentration of the radical species ($[P_n^\bullet]$).[65] Since the rate of polymerization (R_p) is proportional to $[P_n^\bullet]$ and to the square root of $[Cu^{II}Br_2(TPMA)]$, it can be tuned by choosing the appropriate concentration of AsAc (eq 1).[66]

$$R_p = k_p^{app}[M] = k_p[M][P_n^\bullet] = k_p[M]\sqrt{\frac{k_{red}[AsAc][Cu^{II}Br_2(TPMA)]}{k_t}} \quad (1)$$

where $[M]$ is the monomer concentration, k_p is the propagation rate constant, k_{red} is the reduction rate constant of $[Cu^{II}Br_2(TPMA)]$, and k_t is the termination rate constant.

Despite the continuous addition of AsAc, the low overall AsAc concentration (total ratio of $[AsAc]/[Cu^{II}Br_2(TPMA)]$ = 0.5, Table S1, entry 1) did not provide efficient regeneration of the activator. This resulted in a slow polymerization (k_p^{app} = 0.025 h^{-1}), together with a broad dispersity ($Đ$ = 1.70) and low particle brush grafting density ($\sigma \approx 0.11$ nm^{-2}), indicating poor control over the polymerization. A slow polymerization (k_p^{app} = 0.050 h^{-1}) was also observed by initially injecting 0.5 equiv of AsAc (with respect to initial $[Br{-}Cu^{II}(TPMA)]^+$ concentration) at t = 0 h and then subsequently every 1 h (Table S1, entry 4). Nevertheless, due to the sufficient amount of total AsAc added (1.5 equiv to initial $[Br{-}Cu^{II}(TPMA)]^+$ concentration), particle brushes with good polymerization control were achieved with low dispersity ($Đ$ = 1.20) and higher grafting density ($\sigma \approx 0.56$ nm^{-2}). Rapid and well-controlled polymerizations were observed by continuous injection of 0.33−0.50 equiv of AsAc *vs* $[Br{-}Cu^{II}(TPMA)]^+$ per hour (Table S1, entries 2 and 3). Particle brushes with narrow molecular weight distributions ($Đ$ < 1.20) and high grafting densities (σ > 0.75 nm^{-2}) were obtained with good agreement between experimental and theoretical MWs, demonstrating excellent control over polymerization.

In a single-catalyst miniemulsion SI-ARGET ATRP, interparticle brush termination reactions are confined within individual droplets, thus avoiding macroscopic gelation. Therefore, high conversion polymerizations under these conditions are possible, even up to 70% monomer conversion with low dispersity ($Đ$ = 1.20; Table S1, entry 4). The presented method creates the possibility of successful polymerization at a lower temperature (65 °C) and in a much shorter time (3 h) as compared to the previously reported miniemulsion SI-AGET ATRP system (80 °C, 6−20 h).[57] No macroscopic gelation (caused by interparticle brush coupling) was observed, as confirmed by GPC traces of the PBA brush layer etched from silica (Figure S2). Moreover, all

https://doi.org/10.1021/acs.macromol.2c01114
Macromolecules 2022, 55, 6332−6340

precipitated PBA-grafted particle brushes were well redispersed in tetrahydrofuran, showing evenly distributed hybrid silica NPs in TEM. Therefore, ion-pair and interfacial catalysis miniemulsion media facilitated a faster polymerization and prevented macroscopic gelation.

Effect of Catalyst Loadings on Single-Catalyst Miniemulsion SI-ARGET ATRP of BA. The hydrophilicity of the catalyst and the nature of the anionic surfactant greatly affect the ATRP in dispersed media. Since the activator complex, ion pair ($[Cu^{I}(TPMA)]^{+}/[DS]^{-}$), or the neutral complex $Br-Cu^{I}(TPMA)$ may enter the organic phase at concentrations that are only slightly higher than $[Br-Cu^{II}(TPMA)]^{+}/[DS]^{-}$ concentration,[60] it is crucial to optimize the Cu catalyst concentration to achieve good control over the polymerization. The $[Br-Cu^{II}(TPMA)]^{+}$ deactivator loadings varied from 1100 to 750, 400, and 100 ppm (Table 2, entries 1−4) in a miniemulsion SI-ARGET ATRP of BA grafting from silica NPs and resulted in good control of polymerization with narrow distributions ($Đ$ from 1.17 to 1.31). Using only 100 ppm of $[Br-Cu^{II}(TPMA)]^{+}$ in miniemulsion (Table 2, entry 4), we achieved a similar level of control to AGET ATRP with a significantly higher amount of Cu (~2,000 to 4,000 ppm).[57] This represents a 20- to 40-fold decrease in total Cu catalyst concentration.

Control over the polymerization was lost when 75 ppm or lower Cu loadings were used (Table 2, entries 5−9). This was indicated by the increasing dispersity ($1.58 \leq Đ \leq 2.30$) and the decreasing grafting densities ($0.52\ nm^{-2} \geq \sigma \geq 0.07\ nm^{-2}$, Figure 1), meaning insufficient initiation. In our previous work, we studied the tuning dispersities and grafting densities of particle brushes by varying Cu catalyst concentration in SI-ARGET ATRP in an organic solvent.[16] The lowest catalyst amount to maintain good polymerization control was 25 ppm. Below this threshold value, particle brushes with increased $Đ$ and decreased grafting densities were formed. Considering that in the miniemulsion system, the BA monomer with hexadecane composed of the oil phase accounting for *ca.* 24.7 vol %, 100 ppm Cu can be considered as a low threshold value for this system. The ~25 vol %, fourfold Cu also proved the homogeneity of the miniemulsion system, as well as the high transportation and catalytic efficiency, thanks to the interfacial and ion-pair catalysis. For all subsequent miniemulsion SI-ARGET ATRP, 750 ppm Cu catalyst was used, which provided sufficient initiation and good polymerization control.

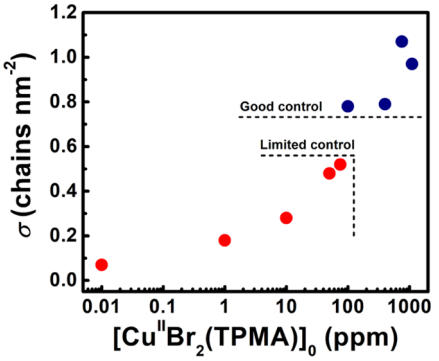

Figure 1. Single-catalyst miniemulsion SI-ARGET ATRP of BA grafting from silica NPs with various catalyst loadings. Grafting densities (σ) *vs* Cu catalyst concentrations (compared to monomer concentration) (red, limited polymerization control; blue, good polymerization control). Reaction conditions are listed in Table 2.

Direct TEM visualization of the core−shell hybrid nanoparticles (750 ppm of the catalyst; Table 2, entry 2) provided additional evidence for an aggregation-free controlled miniemulsion ARGET ATRP. The soft PBA chains formed a shell with uniform size and were clearly distinguished from the rigid silica cores (Figure S3a). Additionally, the uniform size distribution of PBA-grafted SiO_2 NPs was observed with no obvious aggregations by DLS (Figure S3b). In contrast, the use of 0.01 ppm of Cu catalyst resulted in uncontrolled polymerization. TEM imaging revealed the existence of a fraction of particle aggregates with string-like structures formed by the attraction between bare NP surfaces (Figures S3c), which was further confirmed by the uneven size distribution of the particle brushes (Figures S3d).

Effect of Hydroxyl Radicals Generated by Ultrasonication. Grafting density denotes the number of chains grafted from the surface (per square nanometers).[67] In SI-ATRP, the fast initiation by surface-anchored initiators and high livingness of chain ends leads to uniform chain growth, thus a high grafting density. Kinetic studies were performed to determine the brush growth during miniemulsion SI-ARGET ATRP (Table S2, entry 1). While the linear polymerization rate in 3 h indicated that the polymerization proceeded at a steady rate (Figure 2a), the molecular weight (of brush cleaved from silica) as the function of monomer conversion showed a slowing and curved increase (Figure 2b). The nonlinear chain growth at a constant polymerization rate could be attributed to the formation of new polymer chains. Contamination with linear polymers might limit some applications of particle brushes.[5,68] Therefore, the origin of linear polymers was further investigated.

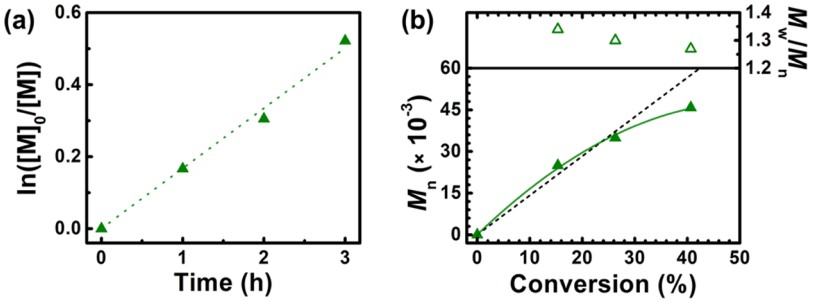

Figure 2. Effect of hydroxyl radicals generated by ultrasonication on miniemulsion SI-ARGET ATRP. (a) Kinetic plots. (b) Evolution of molecular weight (M_n, filled icons) and dispersity ($Đ$, empty icons) of the polymers (after using HF to cleave the silica) as a function of monomer conversion in SI-ARGET ATRP. The black dash line denotes the theoretical M_n. The reaction condition (Table S2, entry 1) is the same as Table 2, entry 2.

https://doi.org/10.1021/acs.macromol.2c01114
Macromolecules 2022, 55, 6332−6340

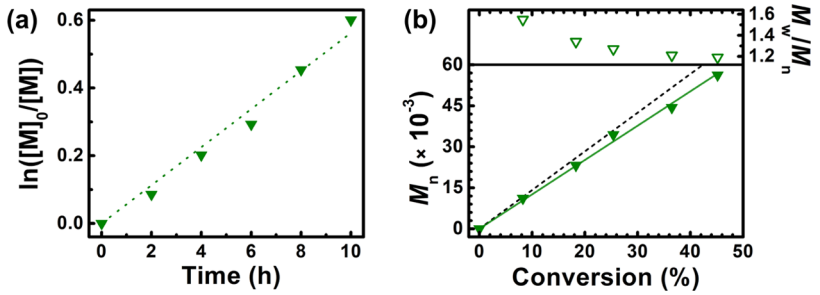

Figure 3. Miniemulsion SI-ARGET ATRP after adding MBF as a hydroxyl radical scavenger. (a) Kinetic plots. (b) Evolution of molecular weight (M_n, filled icons) and dispersity ($Đ$, empty icons) of the polymers (after using HF to cleave the silica) as a function of monomer conversion in the SI-ARGET ATRP. The black dash line denotes the theoretical M_n. The reaction condition is listed in Table S2, entry 2.

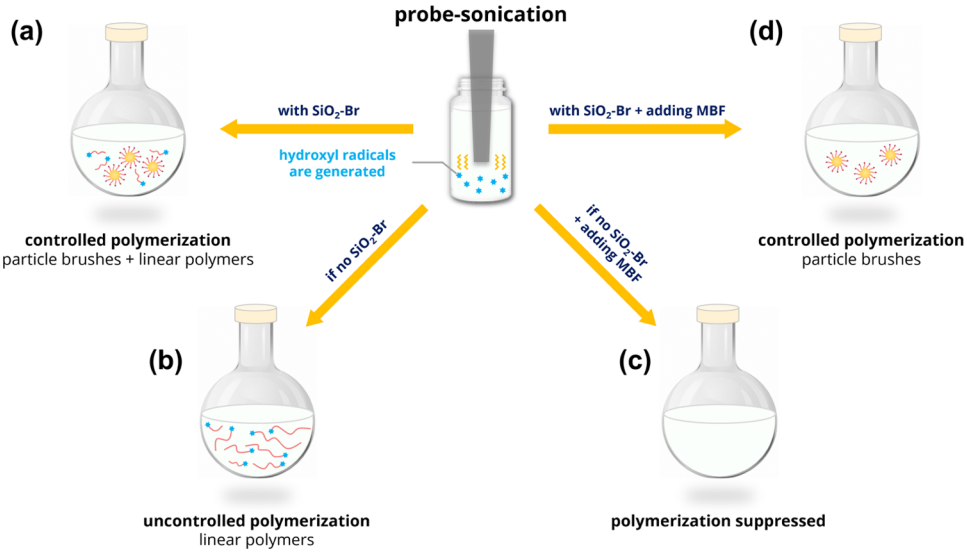

Figure 4. Schematic illustration of the effect of hydroxyl radicals generated by ultrasonication on miniemulsion SI-ARGET ATRP. (a) Hydroxyl radicals functioned as initiators together with SiO_2−Br, leading to mixed linear polymers and particle brushes. (b) Without SiO_2−Br, hydroxyl radicals as the sole initiators led to the formation of linear polymers with broad distributions. (c) Upon MBF addition, hydroxyl radicals were scavenged, and the generation of new polymer chains was significantly suppressed. (d) MBF addition contributed to relatively pure particle brushes initiated by SiO_2−Br.

We hypothesized that the new polymer chains formed as a result of ultrasonication that was used to form the miniemulsion.[69] Ultrasonication in water has already been proven to introduce hydroxyl radicals, which could initiate a reversible addition−fragmentation chain transfer (RAFT) polymerization.[70] In addition to functioning as initiators, hydroxyl radicals have been shown to reduce Cu^{II} complexes, thus triggering ATRP in aqueous media.[71]

To confirm that ultrasonication had no effect on SiO_2−Br, monomer, or solvent (anisole) in a homogeneous SI-ARGET ATRP, control experiments were carried out using intentional ultrasonication on SiO_2−Br dissolved in anisole and SiO_2−Br in monomer, respectively (Table S3). Compared with the conditions where ultrasonication was not applied, no obvious increase in grafting density was observed in both experiments. Considering that hydroxyl radicals could initiate linear polymers, another control experiment was performed in which the SiO_2−Br initiator was excluded without changing the other components of the miniemulsion. After 22 h, the monomer conversion was 20% (Figure S4a,b), and GPC measurements showed polymer elution with broad distributions ($Đ$ = 1.89) as a sign of ATRP with low initiator concentrations (Figure S4c).[72] The generation of hydroxyl radicals by ultrasonication was proposed.

Pyruvic acid and its derivatives (*e.g.*, sodium pyruvate, ethyl pyruvate) have been shown to scavenge reactive oxygen species (ROS), such as superoxide anion radicals, hydrogen peroxide, and hydroxyl radicals.[73] Presumably, in miniemulsion polymerization, hydroxyl radicals generated in water by ultrasonication can be transported into oil droplets. These hydroxyl radicals then initiate new polymer chains along with SiO_2−Br initiating particle brushes. Since pyruvic acid (and pyruvate derivatives) mainly function in the aqueous phase,[74] we use methyl benzoylformate (MBF), which not only has a similar molecular scaffold but is also miscible with monomer and hexadecane in the oil phase.[75] In a subsequent control experiment, MBF was added into the oil phase (with BA and HD, but still excluding SiO_2−Br initiator). Despite using ultrasound to generate the miniemulsion and running the reaction for 22 h, no monomer conversion was observed.

Miniemulsion SI-ARGET ATRP of BA was then repeated with MBF addition (Table S2, entry 2). In the presence of MBF (0.2 M), a much slower polymerization (k_p^{app} = 0.060 h^{-1}) was observed (Figure 3a) compared to conditions without MBF (k_p^{app} = 0.174 h^{-1}). The decreased polymerization rate

https://doi.org/10.1021/acs.macromol.2c01114
Macromolecules 2022, 55, 6332−6340

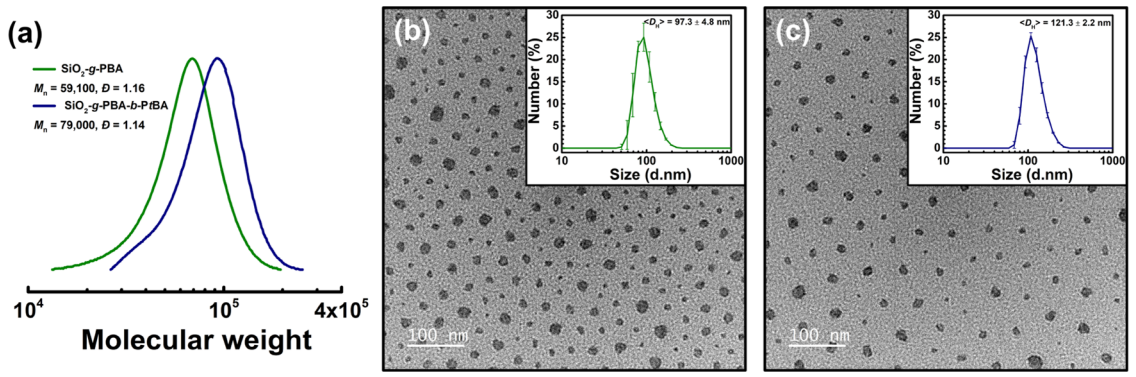

Figure 5. Chain extension of *t*BA from SiO_2-*g*-PBA−Br macroinitiator using miniemulsion SI-ARGET ATRP with MBF as a hydroxyl radical scavenger. (a) GPC analysis of the chain extension from the macroinitiators. Reaction conditions are listed in Table S4. TEM images of monolayer films of (b) SiO_2-*g*-PBA (green) and (c) SiO_2-*g*-PBA-*b*-P*t*BA (blue) nanoparticle brushes (scale bar: 100 nm). Inset: DLS hydrodynamic size distributions by number (in THF).

indicated that MBF effectively scavenged hydroxyl radicals, thus lowering the concentration of propagating radicals. To achieve higher monomer conversion, the polymerization time was increased to 10 h. A steady increase in the linear growth of M_n as a function of monomer conversion was observed (Figure 3b). Well-controlled polymerization was maintained ($Đ$ = 1.19) at 45% monomer conversion. Furthermore, the grafting density was significantly reduced from 0.96 to 0.86 using 750 ppm of Cu catalyst. Overall, in the miniemulsion SI-ARGET ATRP, the slower polymerization, the linear dependence of M_n on conversion, and the lower grafting density indicated that the formation of linear polymers was effectively suppressed by MBF addition.

The effect of hydroxyl radicals on the miniemulsion SI-ARGET ATRP is shown in Figure 4. Hydroxyl radicals were first generated during the ultrasonication for homogenizing miniemulsion. The majority of radicals recombined to form hydrogen peroxide (H_2O_2). Upon degassing with nitrogen and heating, H_2O_2 underwent decomposition into hydroxyl radicals, functioning as initiators together with SiO_2−Br, leading to mixed linear polymers and particle brushes (Figure 4a). Without SiO_2−Br, hydroxyl radicals acted as the sole initiators, leading to uncontrolled polymerization with broad distributions (Figure 4b). In turn, adding MBF, a hydroxyl radical scavenger, inhibited the uncontrolled polymerization (Figure 4c). Consequently, relatively pure particle brushes could be obtained after the addition of MBF (Figure 4d).

Chain Extension of SiO_2-*g*-PBA Brushes. Chain extension of the SiO_2-*g*-PBA−Br macroinitiator was successfully performed using *tert*-butyl acrylate monomer (*t*BA, Table S4, entry 2). The PBA-*b*-P*t*BA brush growth was studied by cleavage from silica and subsequent GPC analysis (Figures 5a and S5). Controlled polymerization was obtained with a steady increase in the MW shift and low $Đ$, confirming the high retention of chain-end functionality in the first PBA block by miniemulsion SI-ARGET ATRP. Macromolecular brushes were formed with a slightly higher grafting density of 0.92 nm^{-2}. This plausibly originated from the hindered dormant polymeric brushes with inaccessible bromides buried inside the propagating chains,[76] thus lowering M_n and influencing the calculation outcome of grafting density. Nevertheless, the grafting density value was similar to previously reported values for polyacrylates-grafted SiO_2 particle brush systems.[38]

DLS indicated the shift in the number-based size distributions of SiO_2-*g*-PBA-*b*-P*t*BA compared with that of the SiO_2-*g*-PBA−Br macroinitiator (Figure 5b,c). The number-average hydrodynamic diameters were $\langle D_H \rangle$ = 121 nm and $\langle D_H \rangle$ = 97 nm, respectively. They shared similarly narrow size distributions with no detectable aggregation (Figure S6), which further supported the fact that the uniform increase in the total hybrid nanoparticle sizes resulted from a well-controlled surface-initiated polymerization. TEM images confirmed the successful grafting of P*t*BA from the macroinitiator. Silica nanoparticles were evenly distributed among the grafted polymer brushes with increasing intervals after chain extension. The random sampling of next-nearest particle spacings based on TEM images for both SiO_2-*g*-PBA and SiO_2-*g*-PBA-*b*-P*t*BA yielded (number average) distances of 41.6 ± 6.9 and 60.1 ± 11.5 nm, respectively (Table S5). To deduce the structure of brush particles, the brush height $h = (\langle D_H \rangle - D_{core})/2$ was correlated with the total degree of polymerization of grafted chains. The analysis revealed $h \sim N^{0.64}$, which indicated "polymer in a good solvent" condition (Table S6). This was indeed consistent with the expected brush architecture that, for both brush particle systems, was expected to be in the semidilute regime.[13,77,78] Hence, the analysis of brush systems confirmed that the brush structure followed the predicted trends for brush particles with the prescribed architecture (σ, N).

■ CONCLUSIONS

Well-defined, densely grafted particle brushes were synthesized from 15.8 nm silica nanoparticles *via* a miniemulsion SI-ARGET ATRP triggered by ascorbic acid under interfacial and ion-pair catalysis conditions. In comparison to previous SI-AGET ATRP in miniemulsion, this single-catalyst system in dispersed media allowed the preparation of hybrid materials at *ca.* 20-fold lower catalyst concentration, *i.e.*, ∼100 ppm of $[Br-Cu^{II}(TPMA)]^+$ in the reaction mixture. The grafting-from polymerization at 65 °C resulted in a high monomer conversion (up to 70%), high grafting densities (*ca.* 0.8 chains nm^{-2}), and low dispersity ($Đ \leq 1.3$). Importantly, no macroscopic gelation was observed. Kinetic studies showed a nonlinear molecular weight increase as a function of monomer conversion. This was attributed to the formation of linear polymers initiated by the hydroxyl radicals generated by ultrasonication. After the addition of methyl benzoylformate, the generation of new polymer chains was suppressed, and relatively pure particle brushes were obtained. This system allowed for chain extension of the grafted PBA brushes with a

https://doi.org/10.1021/acs.macromol.2c01114
Macromolecules 2022, 55, 6332−6340

second P*t*BA block, indicating the high chain-end livingness. Hydrodynamic size distributions by DLS and direct visualization by TEM both illustrated polymer-grafted nanoparticles with high size uniformity, providing additional evidence for the formation of well-defined hybrids. Moreover, the increasing distance between silica nanoparticles observed in TEM also proved the successful grafting of a second block. Dispersions of particle brushes were stable without indication of any nanoparticle aggregation. The interfacial and ion-pair catalysis system offers numerous advantages in the preparation of polymer tethered nanoparticles compared to traditional hydrophobic SI-ARGET ATRP. The polymerizations were carried out using commercially available reagents. High grafting density and better polymerization control were achieved despite the use of a low amount of copper catalyst. Since 95% of the catalyst was bound at the water/oil interface and could be easily removed, we envision that this method may find application in large-scale particle brush fabrication.

■ ASSOCIATED CONTENT

Supporting Information

The Supporting Information is available free of charge at https://pubs.acs.org/doi/10.1021/acs.macromol.2c01114.

Details of experimental procedures; TEM image of miniemulsion droplets; and additional polymerization and characterization results (PDF)

■ AUTHOR INFORMATION

Corresponding Authors

Paweł Chmielarz − *Department of Physical Chemistry, Faculty of Chemistry, Rzeszow University of Technology, 35-959 Rzeszow, Poland; Department of Chemistry, Carnegie Mellon University, Pittsburgh, Pennsylvania 15213, United States;* orcid.org/0000-0002-9101-6264; Email: p_chmiel@prz.edu.pl

Krzysztof Matyjaszewski − *Department of Chemistry, Carnegie Mellon University, Pittsburgh, Pennsylvania 15213, United States;* orcid.org/0000-0003-1960-3402; Email: km3b@andrew.cmu.edu

Authors

Rongguan Yin − *Department of Chemistry, Carnegie Mellon University, Pittsburgh, Pennsylvania 15213, United States;* orcid.org/0000-0002-8956-3226

Izabela Zaborniak − *Department of Physical Chemistry, Faculty of Chemistry, Rzeszow University of Technology, 35-959 Rzeszow, Poland; Department of Chemistry, Carnegie Mellon University, Pittsburgh, Pennsylvania 15213, United States;* orcid.org/0000-0001-7533-3668

Yuqi Zhao − *Department of Materials Science & Engineering, Carnegie Mellon University, Pittsburgh, Pennsylvania 15213, United States;* orcid.org/0000-0002-4438-3635

Grzegorz Szczepaniak − *Department of Chemistry, Carnegie Mellon University, Pittsburgh, Pennsylvania 15213, United States;* orcid.org/0000-0002-0355-9542

Zongyu Wang − *Department of Chemistry, Carnegie Mellon University, Pittsburgh, Pennsylvania 15213, United States*

Tong Liu − *Department of Chemistry, Carnegie Mellon University, Pittsburgh, Pennsylvania 15213, United States*

Yi Wang − *Department of Chemistry, Carnegie Mellon University, Pittsburgh, Pennsylvania 15213, United States*

Mingkang Sun − *Department of Chemistry, Carnegie Mellon University, Pittsburgh, Pennsylvania 15213, United States;* orcid.org/0000-0003-4652-5243

Hanshu Wu − *Department of Materials Science & Engineering, Carnegie Mellon University, Pittsburgh, Pennsylvania 15213, United States*

Jirameth Tarnsangpradit − *Department of Materials Science & Engineering, Carnegie Mellon University, Pittsburgh, Pennsylvania 15213, United States*

Michael R. Bockstaller − *Department of Materials Science & Engineering, Carnegie Mellon University, Pittsburgh, Pennsylvania 15213, United States;* orcid.org/0000-0001-9046-9539

Complete contact information is available at: https://pubs.acs.org/10.1021/acs.macromol.2c01114

Author Contributions

[‖]R.Y. and P.C. contributed equally to this work as co-first authors. The manuscript was written through the contributions of all authors.

Notes

The authors declare no competing financial interest.

■ ACKNOWLEDGMENTS

Financial support from NSF (DMR 2202747, DMR 2209587) and the Department of Energy (DOE-BES-DESC0018854) is gratefully acknowledged. P.C. acknowledges the Ministry of Science and Higher Education scholarship for outstanding young scientists (0001/E-363/STYP/13/2018).

■ REFERENCES

(1) Tsujii, Y.; Ohno, K.; Yamamoto, S.; Goto, A.; Fukuda, T. Structure and Properties of High-Density Polymer Brushes Prepared by Surface-Initiated Living Radical Polymerization. In *Surface-Initiated Polymerization I*; Jordan, R., Ed.; Springer Berlin Heidelberg: Berlin, Heidelberg, 2006; pp 1−45.

(2) Kumar, S. K.; Benicewicz, B. C.; Vaia, R. A.; Winey, K. I. 50th Anniversary Perspective: Are Polymer Nanocomposites Practical for Applications? *Macromolecules* **2017**, *50*, 714−731.

(3) Yan, J.; Bockstaller, M. R.; Matyjaszewski, K. Brush-modified materials: Control of molecular architecture, assembly behavior, properties and applications. *Prog. Polym. Sci.* **2020**, *100*, No. 101180.

(4) Wang, Z.; Bockstaller, M. R.; Matyjaszewski, K. Synthesis and Applications of ZnO/Polymer Nanohybrids. *ACS Mater. Lett.* **2021**, *3*, 599−621.

(5) Bilchak, C. R.; Jhalaria, M.; Huang, Y.; Abbas, Z.; Midya, J.; Benedetti, F. M.; Parisi, D.; Egger, W.; Dickmann, M.; Minelli, M.; Doghieri, F.; Nikoubashman, A.; Durning, C. J.; Vlassopoulos, D.; Jestin, J.; Smith, Z. P.; Benicewicz, B. C.; Rubinstein, M.; Leibler, L.; Kumar, S. K. Tuning Selectivities in Gas Separation Membranes Based on Polymer-Grafted Nanoparticles. *ACS Nano* **2020**, *14*, 17174−17183.

(6) Hui, C. M.; Pietrasik, J.; Schmitt, M.; Mahoney, C.; Choi, J.; Bockstaller, M. R.; Matyjaszewski, K. Surface-Initiated Polymerization as an Enabling Tool for Multifunctional (Nano-)Engineered Hybrid Materials. *Chem. Mater.* **2014**, *26*, 745−762.

(7) Wu, L.; Glebe, U.; Böker, A. Synthesis of Hybrid Silica Nanoparticles Densely Grafted with Thermo and pH Dual-Responsive Brushes via Surface-Initiated ATRP. *Macromolecules* **2016**, *49*, 9586−9596.

(8) Han, J.; Zhai, Y.; Wang, Z.; Bleuel, M.; Liu, T.; Yin, R.; Wu, W.; Hakem, I. F.; Karim, A.; Matyjaszewski, K.; Bockstaller, M. R. Nanosized Organo-Silica Particles with "Built-In" Surface-Initiated Atom Transfer Radical Polymerization Capability as a Platform for Brush Particle Synthesis. *ACS Macro Lett.* **2020**, *9*, 1218−1223.

(9) Yuan, C.; Käfer, F.; Ober, C. K. Polymer-Grafted Nanoparticles (PGNs) with Adjustable Graft-Density and Interparticle Hydrogen Bonding Interaction. *Macromol. Rapid Commun.* **2022**, *43*, No. 2100629.
(10) Zhu, T.; Rahman, M. A.; Benicewicz, B. C. Synthesis of Well-Defined Polyolefin Grafted SiO_2 Nanoparticles with Molecular Weight and Graft Density Control. *ACS Macro Lett.* **2020**, *9*, 1255−1260.
(11) Zoppe, J. O.; Ataman, N. C.; Mocny, P.; Wang, J.; Moraes, J.; Klok, H.-A. Surface-Initiated Controlled Radical Polymerization: State-of-the-Art, Opportunities, and Challenges in Surface and Interface Engineering with Polymer Brushes. *Chem. Rev.* **2017**, *117*, 1105−1318.
(12) Li, F.; Thiele, S.; Klok, H.-A. Polymethylene Brushes via Surface-Initiated C1 Polyhomologation. *J. Am. Chem. Soc.* **2021**, *143*, 19873−19880.
(13) Ohno, K.; Morinaga, T.; Takeno, S.; Tsujii, Y.; Fukuda, T. Suspensions of Silica Particles Grafted with Concentrated Polymer Brush: Effects of Graft Chain Length on Brush Layer Thickness and Colloidal Crystallization. *Macromolecules* **2007**, *40*, 9143−9150.
(14) Yin, R.; Wang, Z.; Bockstaller, M. R.; Matyjaszewski, K. Tuning dispersity of linear polymers and polymeric brushes grown from nanoparticles by atom transfer radical polymerization. *Polym. Chem.* **2021**, *12*, 6071−6082.
(15) Li, T.-H.; Yadav, V.; Conrad, J. C.; Robertson, M. L. Effect of Dispersity on the Conformation of Spherical Polymer Brushes. *ACS Macro Lett.* **2021**, *10*, 518−524.
(16) Wang, Z.; Yan, J.; Liu, T.; Wei, Q.; Li, S.; Olszewski, M.; Wu, J.; Sobieski, J.; Fantin, M.; Bockstaller, M. R.; Matyjaszewski, K. Control of Dispersity and Grafting Density of Particle Brushes by Variation of ATRP Catalyst Concentration. *ACS Macro Lett.* **2019**, *8*, 859−864.
(17) Wang, Z.; Liu, T.; Zhao, Y.; Lee, J.; Wei, Q.; Yan, J.; Li, S.; Olszewski, M.; Yin, R.; Zhai, Y.; Bockstaller, M. R.; Matyjaszewski, K. Synthesis of Gradient Copolymer Grafted Particle Brushes by ATRP. *Macromolecules* **2019**, *52*, 9466−9475.
(18) Wang, Z.; Lee, J.; Wang, Z.; Zhao, Y.; Yan, J.; Lin, Y.; Li, S.; Liu, T.; Olszewski, M.; Pietrasik, J.; Bockstaller, M. R.; Matyjaszewski, K. Tunable Assembly of Block Copolymer Tethered Particle Brushes by Surface-Initiated Atom Transfer Radical Polymerization. *ACS Macro Lett.* **2020**, *9*, 806−812.
(19) Chremos, A.; Douglas, J. F. Self-assembly of polymer-grafted nanoparticles in solvent-free conditions. *Soft Matter* **2016**, *12*, 9527−9537.
(20) Yan, J.; Kristufek, T.; Schmitt, M.; Wang, Z.; Xie, G.; Dang, A.; Hui, C. M.; Pietrasik, J.; Bockstaller, M. R.; Matyjaszewski, K. Matrix-free Particle Brush System with Bimodal Molecular Weight Distribution Prepared by SI-ATRP. *Macromolecules* **2015**, *48*, 8208−8218.
(21) Lee, J.; Wang, Z.; Zhang, J.; Yan, J.; Deng, T.; Zhao, Y.; Matyjaszewski, K.; Bockstaller, M. R. Molecular Parameters Governing the Elastic Properties of Brush Particle Films. *Macromolecules* **2020**, *53*, 1502−1513.
(22) Bohannon, C. A.; Chancellor, A. J.; Kelly, M. T.; Le, T. T.; Zhu, L.; Li, C. Y.; Zhao, B. Adaptable Multivalent Hairy Inorganic Nanoparticles. *J. Am. Chem. Soc.* **2021**, *143*, 16919−16924.
(23) Li, S.; Liu, T.; Yan, J.; Flum, J.; Wang, H.; Lorandi, F.; Wang, Z.; Fu, L.; Hu, L.; Zhao, Y.; Yuan, R.; Sun, M.; Whitacre, J. F.; Matyjaszewski, K. Grafting polymer from oxygen-vacancy-rich nanoparticles to enable protective layers for stable lithium metal anode. *Nano Energy* **2020**, *76*, No. 105046.
(24) Wåhlander, M.; Nilsson, F.; Andersson, R. L.; Sanchez, C. C.; Taylor, N.; Carlmark, A.; Hillborg, H.; Malmström, E. Tailoring dielectric properties using designed polymer-grafted ZnO nanoparticles in silicone rubber. *J. Mater. Chem. A* **2017**, *5*, 14241−14258.
(25) Yavuz, M. S.; Cheng, Y.; Chen, J.; Cobley, C. M.; Zhang, Q.; Rycenga, M.; Xie, J.; Kim, C.; Song, K. H.; Schwartz, A. G.; Wang, L. V.; Xia, Y. Gold nanocages covered by smart polymers for controlled release with near-infrared light. *Nat. Mater.* **2009**, *8*, 935−939.
(26) Pageni, P.; Yang, P.; Chen, Y. P.; Huang, Y.; Bam, M.; Zhu, T.; Nagarkatti, M.; Benicewicz, B. C.; Decho, A. W.; Tang, C. Charged Metallopolymer-Grafted Silica Nanoparticles for Antimicrobial Applications. *Biomacromolecules* **2018**, *19*, 417−425.
(27) Tao, P.; Li, Y.; Siegel, R. W.; Schadler, L. S. Transparent luminescent silicone nanocomposites filled with bimodal PDMS-brush-grafted CdSe quantum dots. *J. Mater. Chem. C* **2013**, *1*, 86−94.
(28) Williams, G. A.; Ishige, R.; Cromwell, O. R.; Chung, J.; Takahara, A.; Guan, Z. Mechanically Robust and Self-Healable Superlattice Nanocomposites by Self-Assembly of Single-Component "Sticky" Polymer-Grafted Nanoparticles. *Adv. Mater.* **2015**, *27*, 3934−3941.
(29) Wright, R. A. E.; Wang, K.; Qu, J.; Zhao, B. Oil-Soluble Polymer Brush Grafted Nanoparticles as Effective Lubricant Additives for Friction and Wear Reduction. *Angew. Chem.* **2016**, *128*, 8798−8802.
(30) Kawata, Y.; Yamamoto, T.; Kihara, H.; Ohno, K. Dual Self-Healing Abilities of Composite Gels Consisting of Polymer-Brush-Afforded Particles and an Azobenzene-Doped Liquid Crystal. *ACS Appl. Mater. Interfaces* **2015**, *7*, 4185−4191.
(31) Matyjaszewski, K.; Dong, H.; Jakubowski, W.; Pietrasik, J.; Kusumo, A. Grafting from Surfaces for "Everyone": ARGET ATRP in the Presence of Air. *Langmuir* **2007**, *23*, 4528−4531.
(32) Matyjaszewski, K. Advanced Materials by Atom Transfer Radical Polymerization. *Adv. Mater.* **2018**, *30*, No. 1706441.
(33) Khabibullin, A.; Mastan, E.; Matyjaszewski, K.; Zhu, S. Surface-Initiated Atom Transfer Radical Polymerization. In *Controlled Radical Polymerization at and from Solid Surfaces*; Vana, P., Ed.; Springer International Publishing: Cham, 2016; pp 29−76.
(34) Pyun, J.; Kowalewski, T.; Matyjaszewski, K. Synthesis of Polymer Brushes Using Atom Transfer Radical Polymerization. *Macromol. Rapid Commun.* **2003**, *24*, 1043−1059.
(35) Parkatzidis, K.; Wang, H. S.; Truong, N. P.; Anastasaki, A. Recent Developments and Future Challenges in Controlled Radical Polymerization: A 2020 Update. *Chem* **2020**, *6*, 1575−1588.
(36) Corrigan, N.; Jung, K.; Moad, G.; Hawker, C. J.; Matyjaszewski, K.; Boyer, C. Reversible-deactivation radical polymerization (Controlled/living radical polymerization): From discovery to materials design and applications. *Prog. Polym. Sci.* **2020**, *111*, No. 101311.
(37) Fromel, M.; Benetti, E. M.; Pester, C. W. Oxygen Tolerance in Surface-Initiated Reversible Deactivation Radical Polymerizations: Are Polymer Brushes Turning into Technology? *ACS Macro Lett.* **2022**, *11*, 415−421.
(38) Chmielarz, P.; Yan, J.; Krys, P.; Wang, Y.; Wang, Z.; Bockstaller, M. R.; Matyjaszewski, K. Synthesis of Nanoparticle Copolymer Brushes via Surface-Initiated *se*ATRP. *Macromolecules* **2017**, *50*, 4151−4159.
(39) Jakubowski, W.; Min, K.; Matyjaszewski, K. Activators Regenerated by Electron Transfer for Atom Transfer Radical Polymerization of Styrene. *Macromolecules* **2006**, *39*, 39−45.
(40) Jakubowski, W.; Matyjaszewski, K. Activators Regenerated by Electron Transfer for Atom-Transfer Radical Polymerization of (Meth)acrylates and Related Block Copolymers. *Angew. Chem., Int. Ed.* **2006**, *45*, 4482−4486.
(41) Casolari, R.; Felluga, F.; Frenna, V.; Ghelfi, F.; Pagnoni, U. M.; Parsons, A. F.; Spinelli, D. A green way to γ-lactams through a copper catalyzed ARGET-ATRC in ethanol and in the presence of ascorbic acid. *Tetrahedron* **2011**, *67*, 408−416.
(42) Paterson, S. M.; Brown, D. H.; Chirila, T. V.; Keen, I.; Whittaker, A. K.; Baker, M. V. The synthesis of water-soluble PHEMA via ARGET ATRP in protic media. *J. Polym. Sci., Part A: Polym. Chem.* **2010**, *48*, 4084−4092.
(43) Matyjaszewski, K.; Jakubowski, W.; Min, K.; Tang, W.; Huang, J.; Braunecker Wade, A.; Tsarevsky Nicolay, V. Diminishing catalyst concentration in atom transfer radical polymerization with reducing agents. *Proc. Natl. Acad. Sci. U.S.A.* **2006**, *103*, 15309−15314.
(44) Kwak, Y.; Matyjaszewski, K. ARGET ATRP of methyl methacrylate in the presence of nitrogen-based ligands as reducing agents. *Polym. Int.* **2009**, *58*, 242−247.

https://doi.org/10.1021/acs.macromol.2c01114
Macromolecules 2022, 55, 6332−6340

(45) Chen, H.; Liu, D.; Song, Y.; Qu, R.; Wang, C. ARGET ATRP of acrylonitrile with ionic liquid as reaction media and 1,1,4,7,7-pentamethyldiethylenetriamine as both ligand and reducing agent in the presence of air. *Polym. Adv. Technol.* **2011**, *22*, 1513−1517.
(46) Gnanou, Y.; Hizal, G. Effect of phenol and derivatives on atom transfer radical polymerization in the presence of air. *J. Polym. Sci., Part A: Polym. Chem.* **2004**, *42*, 351−359.
(47) Williams, V. A.; Ribelli, T. G.; Chmielarz, P.; Park, S.; Matyjaszewski, K. A Silver Bullet: Elemental Silver as an Efficient Reducing Agent for Atom Transfer Radical Polymerization of Acrylates. *J. Am. Chem. Soc.* **2015**, *137*, 1428−1431.
(48) Chmielarz, P. Synthesis of inositol-based star polymers through low ppm ATRP methods. *Polym. Adv. Technol.* **2017**, *28*, 1804−1812.
(49) Wei, Q.; Sun, M.; Lorandi, F.; Yin, R.; Yan, J.; Liu, T.; Kowalewski, T.; Matyjaszewski, K. Cu-Catalyzed Atom Transfer Radical Polymerization in the Presence of Liquid Metal Micro/Nanodroplets. *Macromolecules* **2021**, *54*, 1631−1638.
(50) Whitfield, R.; Parkatzidis, K.; Rolland, M.; Truong, N. P.; Anastasaki, A. Tuning Dispersity by Photoinduced Atom Transfer Radical Polymerisation: Monomodal Distributions with ppm Copper Concentration. *Angew. Chem.* **2019**, *131*, 13457−13462.
(51) Wang, Z.; Lorandi, F.; Fantin, M.; Wang, Z.; Yan, J.; Wang, Z.; Xia, H.; Matyjaszewski, K. Atom Transfer Radical Polymerization Enabled by Sonochemically Labile Cu-carbonate Species. *ACS Macro Lett.* **2019**, *8*, 161−165.
(52) Cheng, C.-H.; Masuda, S.; Nozaki, S.; Nagano, C.; Hirai, T.; Kojio, K.; Takahara, A. Fabrication and Deformation of Mechanochromic Nanocomposite Elastomers Based on Rubbery and Glassy Block Copolymer-Grafted Silica Nanoparticles. *Macromolecules* **2020**, *53*, 4541−4551.
(53) Ohno, K.; Morinaga, T.; Koh, K.; Tsujii, Y.; Fukuda, T. Synthesis of Monodisperse Silica Particles Coated with Well-Defined, High-Density Polymer Brushes by Surface-Initiated Atom Transfer Radical Polymerization. *Macromolecules* **2005**, *38*, 2137−2142.
(54) Pietrasik, J.; Hui, C. M.; Chaladaj, W.; Dong, H.; Choi, J.; Jurczak, J.; Bockstaller, M. R.; Matyjaszewski, K. Silica-Polymethacrylate Hybrid Particles Synthesized Using High-Pressure Atom Transfer Radical Polymerization. *Macromol. Rapid Commun.* **2011**, *32*, 295−301.
(55) Min, K.; Gao, H.; Yoon, J. A.; Wu, W.; Kowalewski, T.; Matyjaszewski, K. One-Pot Synthesis of Hairy Nanoparticles by Emulsion ATRP. *Macromolecules* **2009**, *42*, 1597−1603.
(56) Wu, D.-Y.; Käfer, F.; Diaco, N.; Ober, C. K. Silica-PMMA hairy nanoparticles prepared via phase transfer-assisted aqueous miniemulsion atom transfer radical polymerization. *J. Polym. Sci.* **2020**, *58*, 2310−2316.
(57) Bombalski, L.; Min, K.; Dong, H.; Tang, C.; Matyjaszewski, K. Preparation of Well-Defined Hybrid Materials by ATRP in Miniemulsion. *Macromolecules* **2007**, *40*, 7429−7432.
(58) Szczepaniak, G.; Piątkowski, J.; Nogaś, W.; Lorandi, F.; Yerneni, S. S.; Fantin, M.; Ruszczyńska, A.; Enciso, A. E.; Bulska, E.; Grela, K.; Matyjaszewski, K. An isocyanide ligand for the rapid quenching and efficient removal of copper residues after Cu/TEMPO-catalyzed aerobic alcohol oxidation and atom transfer radical polymerization. *Chem. Sci.* **2020**, *11*, 4251−4262.
(59) Shen, Y.; Tang, H.; Ding, S. Catalyst separation in atom transfer radical polymerization. *Prog. Polym. Sci.* **2004**, *29*, 1053−1078.
(60) Fantin, M.; Chmielarz, P.; Wang, Y.; Lorandi, F.; Isse, A. A.; Gennaro, A.; Matyjaszewski, K. Harnessing the Interaction between Surfactant and Hydrophilic Catalyst To Control *e*ATRP in Miniemulsion. *Macromolecules* **2017**, *50*, 3726−3732.
(61) Wang, Y.; Lorandi, F.; Fantin, M.; Chmielarz, P.; Isse, A. A.; Gennaro, A.; Matyjaszewski, K. Miniemulsion ARGET ATRP via Interfacial and Ion-Pair Catalysis: From ppm to ppb of Residual Copper. *Macromolecules* **2017**, *50*, 8417−8425.
(62) Teo, V. L.; Davis, B. J.; Tsarevsky, N. V.; Zetterlund, P. B. Successful Miniemulsion ATRP Using an Anionic Surfactant: Minimization of Deactivator Loss by Addition of a Halide Salt. *Macromolecules* **2014**, *47*, 6230−6237.
(63) Averick, S.; Simakova, A.; Park, S.; Konkolewicz, D.; Magenau, A. J. D.; Mehl, R. A.; Matyjaszewski, K. ATRP under Biologically Relevant Conditions: Grafting from a Protein. *ACS Macro Lett.* **2012**, *1*, 6−10.
(64) Min, K.; Gao, H.; Matyjaszewski, K. Use of Ascorbic Acid as Reducing Agent for Synthesis of Well-Defined Polymers by ARGET ATRP. *Macromolecules* **2007**, *40*, 1789−1791.
(65) Woodruff, S. R.; Davis, B. J.; Tsarevsky, N. V. Epoxides as Reducing Agents for Low-Catalyst-Concentration Atom Transfer Radical Polymerization. *Macromol. Rapid Commun.* **2014**, *35*, 186−192.
(66) Lorandi, F.; Matyjaszewski, K. Why Do We Need More Active ATRP Catalysts? *Isr. J. Chem.* **2020**, *60*, 108−123.
(67) Michalek, L.; Barner, L.; Barner-Kowollik, C. Polymer on Top: Current Limits and Future Perspectives of Quantitatively Evaluating Surface Grafting. *Adv. Mater.* **2018**, *30*, No. 1706321.
(68) Bilchak, C. R.; Buenning, E.; Asai, M.; Zhang, K.; Durning, C. J.; Kumar, S. K.; Huang, Y.; Benicewicz, B. C.; Gidley, D. W.; Cheng, S.; Sokolov, A. P.; Minelli, M.; Doghieri, F. Polymer-Grafted Nanoparticle Membranes with Controllable Free Volume. *Macromolecules* **2017**, *50*, 7111−7120.
(69) Tomovska, R.; de la Cal, J. C.; Asua, J. M.Reactions in Heterogeneous Media. In *Monitoring Polymerization Reactions: From Fundamentals to Applications*; Reed, W. F.; Alb, A. M., Eds.; John Wiley & Sons, Inc., 2013; pp 59−77.
(70) McKenzie, T. G.; Colombo, E.; Fu, Q.; Ashokkumar, M.; Qiao, G. G. Sono-RAFT Polymerization in Aqueous Medium. *Angew. Chem., Int. Ed.* **2017**, *56*, 12302−12306.
(71) Wang, Z.; Wang, Z.; Pan, X.; Fu, L.; Lathwal, S.; Olszewski, M.; Yan, J.; Enciso, A. E.; Wang, Z.; Xia, H.; Matyjaszewski, K. Ultrasonication-Induced Aqueous Atom Transfer Radical Polymerization. *ACS Macro Lett.* **2018**, *7*, 275−280.
(72) Wang, Z.; Fantin, M.; Sobieski, J.; Wang, Z.; Yan, J.; Lee, J.; Liu, T.; Li, S.; Olszewski, M.; Bockstaller, M. R.; Matyjaszewski, K. Pushing the Limit: Synthesis of SiO_2-*g*-PMMA/PS Particle Brushes via ATRP with Very Low Concentration of Functionalized SiO_2−Br Nanoparticles. *Macromolecules* **2019**, *52*, 8713−8723.
(73) Kładna, A.; Marchlewicz, M.; Piechowska, T.; Kruk, I.; Aboul-Enein, H. Y. Reactivity of pyruvic acid and its derivatives towards reactive oxygen species. *Luminescence* **2015**, *30*, 1153−1158.
(74) Szczepaniak, G.; Łagodzińska, M.; Dadashi-Silab, S.; Gorczyński, A.; Matyjaszewski, K. Fully oxygen-tolerant atom transfer radical polymerization triggered by sodium pyruvate. *Chem. Sci.* **2020**, *11*, 8809−8816.
(75) He, X.; Gao, Y.; Nie, J.; Sun, F. Methyl Benzoylformate Derivative Norrish Type I Photoinitiators for Deep-Layer Photocuring under Near-UV or Visible LED. *Macromolecules* **2021**, *54*, 3854−3864.
(76) Arraez, F. J.; Van Steenberge, P. H. M.; Sobieski, J.; Matyjaszewski, K.; D'hooge, D. R. Conformational Variations for Surface-Initiated Reversible Deactivation Radical Polymerization: From Flat to Curved Nanoparticle Surfaces. *Macromolecules* **2021**, *54*, 8270−8288.
(77) Choi, J.; Dong, H.; Matyjaszewski, K.; Bockstaller, M. R. Flexible Particle Array Structures by Controlling Polymer Graft Architecture. *J. Am. Chem. Soc.* **2010**, *132*, 12537−12539.
(78) Dukes, D.; Li, Y.; Lewis, S.; Benicewicz, B.; Schadler, L.; Kumar, S. K. Conformational Transitions of Spherical Polymer Brushes: Synthesis, Characterization, and Theory. *Macromolecules* **2010**, *43*, 1564−1570.

https://doi.org/10.1021/acs.macromol.2c01114
Macromolecules 2022, 55, 6332−6340